

LARGE-SCALE MASS POWER SPECTRUM FROM PECULIAR VELOCITIES

Idit Zehavi^{1,2}

¹*Racah Institute of Physics, The Hebrew University,
Jerusalem 91904, Israel*

²*NASA/Fermilab Astrophysics Group, Fermi National Accelerator
Laboratory, Box 500, Batavia, IL 60510-0500, USA*

ABSTRACT. The power spectrum of mass density fluctuations is estimated from the Mark III and the SFI catalogs of peculiar velocities by applying a maximum likelihood analysis, using parametric models for the power spectrum and for the errors. Generalized CDM models with and without COBE normalization are used. The applications to the two different data sets give consistent results. The general result is a relatively high amplitude of the power spectrum, e.g. at $k = 0.1 h \text{Mpc}^{-1}$ we find $P(k)\Omega^{1.2} = (4.5 \pm 2.0) \times 10^3 (h^{-1}\text{Mpc})^3$, corresponding to $\sigma_8\Omega^{0.6} = 0.85 \pm 0.2$. Model-dependent constraints on combinations of cosmological parameters are obtained for families of COBE-normalized CDM models. These can roughly be approximated by $\Omega h_{60}^\mu n^\nu = 0.6 \pm 0.2$, where $\mu = 1.3$ and $\nu = 3.7, 2.0$ for flat Λ CDM models with and without tensor fluctuations respectively. For open CDM, without tensor fluctuations, the powers are $\mu = 0.9$ and $\nu = 1.4$. The quoted error-bars reflect the 90% formal likelihood uncertainty for each model and the variance among different models and between catalogs. This is a brief review of a collaborative project (for more details, see Zaroubi *et al.* 1997, Freudling *et al.* 1998). Preliminary constraints in the $\Omega - \Omega_\Lambda$ plane are presented as well.

1 Introduction

In the standard picture of cosmology, structure evolved from small density fluctuations that grew by gravitational instability. These initial fluctuations are assumed to have a Gaussian distribution characterized by the power spectrum (PS). On large scales, the fluctuations are linear even at late times and still governed by the initial PS. The PS is thus a useful statistic for large-scale structure, providing constraints on cosmology and theories of structure formation.

The galaxy PS has been estimated in recent years from several redshift surveys (see reviews by Strauss & Willick 1995; Strauss 1998). Alternatively, one can estimate the PS using measurements of peculiar velocities, which are directly related to the *mass* density fluctuations. Velocities are also sensitive to larger scales and thus subject to weaker non-linear effects. In this work, we develop and apply a likelihood analysis (first proposed by Kaiser 1988) in order to estimate the mass PS from peculiar

velocity catalogs. The method, acting on the “raw” peculiar velocities without additional processing, utilizes much of the information content of the data. It takes into account properly the measurement errors and the finite discrete sampling. The simplifying assumptions made are that the velocities follow a Gaussian distribution and that their correlations can be derived from the density PS using linear theory.

Two catalogs are used for this purpose. One is the Mark III catalog of peculiar velocities, a compilation of several data sets, consisting of roughly 3000 spiral and elliptical galaxies within a volume of $\sim 80 h^{-1}\text{Mpc}$ around the local group, grouped into ~ 1200 objects (Willick *et al.* 1995, 1996 1997). The other is the recently completed SFI catalog, a homogeneously selected sample of ~ 1300 spiral field galaxies, designed to minimize effects of combining disparate data sets (Haynes *et al.* 1998; Wegner *et al.* 1998). In both catalogs, the typical relative distance errors of individual galaxies are 15–20%, and both data sets are carefully corrected

for the various systematic biases. It is interesting to compare the results of the two catalogs, especially in view of apparent discrepancies in the appearance of the velocity fields (e.g, da Costa *et al.* 1996, 1998).

2 Method

Given a data set \mathbf{d} , the goal is to estimate the most likely model \mathbf{m} . Invoking a Bayesian approach (and assuming a uniform prior), this can be turned to maximizing the likelihood function $\mathcal{L} \equiv \mathcal{P}(\mathbf{d}|\mathbf{m})$, the probability of the data given the model, as a function of the model parameters. Under the assumption that both the underlying velocities and the observational errors are Gaussian random fields, the likelihood function can be written as

$$\mathcal{L} = [(2\pi)^N \det(R)]^{-1/2} \times \exp \left(-\frac{1}{2} \sum_{i,j}^N d_i R_{ij}^{-1} d_j \right),$$

where $\{d_i\}_{i=1}^N$ is the set of observed peculiar velocities and R is their correlation matrix. R involves the theoretical correlation, calculated in linear theory for each assumed cosmological model, and the estimated covariance of the errors.

The likelihood analysis is performed by choosing some parametric functional form for the PS. Going over the parameter space and calculating the likelihoods for the different models, one finds the PS parameters for which the maximum likelihood is obtained. Confidence levels are estimated by approximating $-2\ln\mathcal{L}$ as a χ^2 distribution with respect to the model parameters. Note that this method, based on peculiar velocities, essentially measures $f(\Omega)^2 P(k)$ and not the mass density PS by itself. We extensively test the method using realistic mock catalogs, designed to mimic in detail the real catalogs (Kolatt *et al.* 1996; El-dar *et al.* 1998).

We use several models for the PS. One of these is the so-called Γ model, where we vary the amplitude and the shape-parameter Γ . The main analysis is done with a suit of generalized CDM models, normalized by the

COBE 4-year data. These include open models, flat models with a cosmological constant and tilted models with or without a tensor component. The free parameters are then the mass-density parameter Ω , the Hubble parameter h and the power index n .

Here, as in any method for estimating the PS, the recovered PS is sensitive to the assumed observational errors, that enter as well the correlation matrix R . To alleviate this problem, we extend the method such that also the magnitude of these errors is determined by the likelihood analysis. This is done by adding free parameters that govern a global change of the assumed errors, in addition to modeling the PS, and provides some reliability check of the magnitude of the errors. We find, for both catalogs, a good agreement with the original error estimates, thus allowing for a more reliable recovery of the PS.

3 Results

Figure 1 shows, as a typical example, the results for the COBE-normalized flat Λ CDM family of models, with a tensor component in the initial fluctuations, when setting $h = 0.6$ and varying Ω and n . Shown are $\ln\mathcal{L}$ contours for the SFI catalog and for Mark III. As can be seen from the elongated contours, what is determined well is not a specific point but a high likelihood ridge, constraining a degenerate combination of the parameters roughly of the form $\Omega n^{3.7} = 0.59 \pm 0.08$, in this case. The corresponding best-fit PS for the two catalogs is presented as well, with the shaded region illustrating the 90% confidence region obtained from the SFI high-likelihood ridge.

These results are representative for all other PS models we tried. For each catalog, the different models yield similar best-fit PS, falling well within each others formal uncertainties and agreeing especially well on intermediate scales ($k \sim 0.1 h \text{ Mpc}^{-1}$). The similarity of the PS obtained from SFI with that of Mark III, which is seen in the figure, is illustrative of the other models as well. This indicates that the

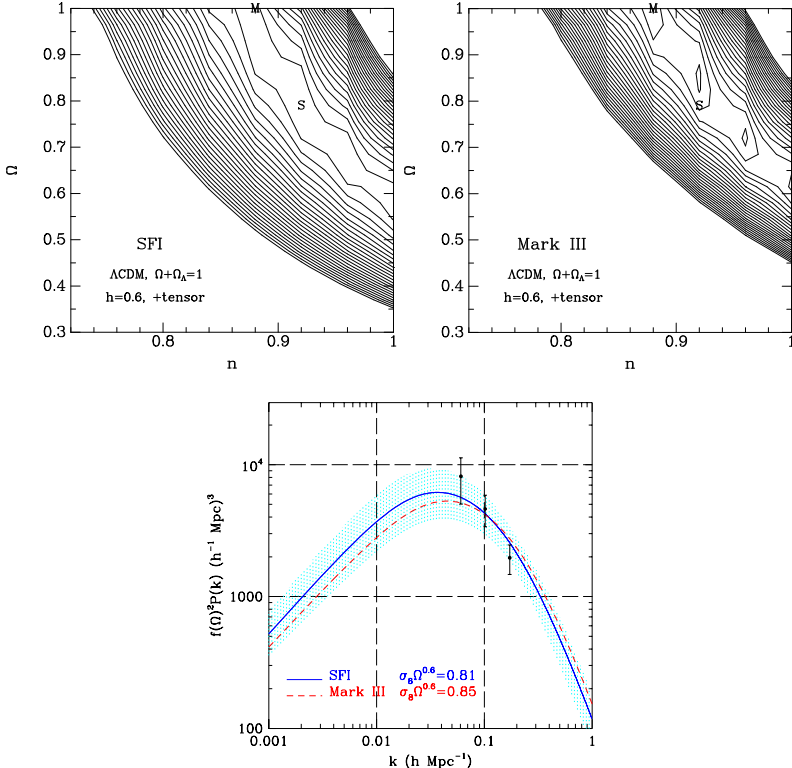


Figure 1. Likelihood analysis results for the COBE-normalized flat Λ CDM model with $h = 0.6$. Shown are $\ln\mathcal{L}$ contours in the $\Omega - n$ plane for SFI (top left panel) and for Mark III (top right). The best-fit parameters for SFI and Mark III are marked, on both, by ‘S’ and ‘M’ respectively. The lower panel shows the corresponding maximum-likelihood PS for SFI (solid line) and for Mark III (dashed). The shaded region is the SFI 90% confidence region. The three solid dots mark the PS calculated from Mark III by Kolatt and Dekel (1997), together with their quoted 1σ error-bar.

peculiar velocities of the two catalogs, with their respective error estimates, are consistent with arising from the same underlying mass density PS. This does not preclude possible differences that are not picked up by this statistic, but can be viewed as another indication of the robustness of the results. Note also the agreement with an independent measure of the PS from the Mark III catalog, using the smoothed density field recovered by POTENT (the three dots; Kolatt & Dekel 1997).

The robust result, for both catalogs and all models, is a relatively high PS, with $P(k)\Omega^{1.2} = (4.5 \pm 2.0) \times 10^3 (h^{-1} \text{Mpc})^3$ at $k = 0.1 h \text{Mpc}^{-1}$. An extrapolation to smaller scales using the different

CDM models gives $\sigma_8\Omega^{0.6} = 0.85 \pm 0.2$. (Such values are also obtained when assuming for the PS the Γ model or the generalized CDM models with a *free* amplitude.) The high-likelihood ridge is a feature of all COBE-normalized CDM models. The general constraints on the combination of cosmological parameters is of the sort $\Omega h_{60}^\mu n^\nu = 0.6 \pm 0.2$, where $\mu = 1.3$ and $\nu = 3.7, 2.0$ for flat Λ CDM models with and without tensor fluctuations respectively. For open CDM, without tensor fluctuations, the powers are $\mu = 0.9$ and $\nu = 1.4$. For the span of models checked, the PS peak is in the range $0.02 \leq k \leq 0.06 h \text{Mpc}^{-1}$. The shape parameter of the Γ model is only weakly constrained to $\Gamma = 0.4 \pm 0.2$.

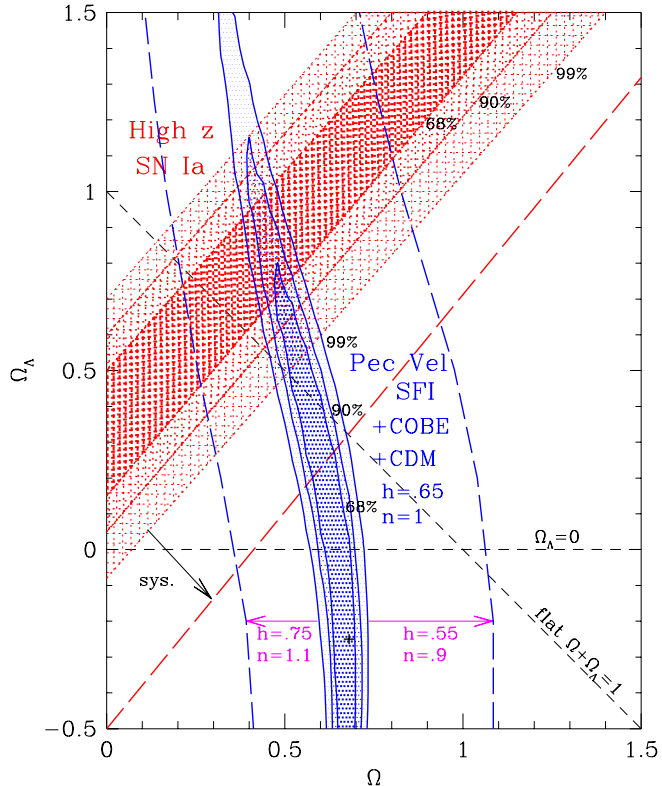


Figure 2. Constraints in the $\Omega - \Omega_\Lambda$ plane coming from a likelihood analysis of the SFI peculiar velocities (the approx. vertical contours) and from the high-redshift SNe Ia (the diagonal contours; Perlmutter *et al.* 1998). The 68, 90 and 99% confidence regions are shown for both. The estimated worst-case systematic error of the SNe results is denoted by the corresponding dashed line. The SFI likelihood contours are for the case of $n = 1$, $h = 0.65$. The shifted dashed lines illustrate the estimated effect of changing the values of these parameters (Zehavi & Dekel 1998).

These error-bars are crude, reflecting the 90% formal likelihood uncertainty for each model, the variance among different models and between catalogs. Care should also be given to possible systematics that could still plague the results, arising perhaps from non-linear effects or some peculiarities in the data (Freudling *et al.* 1998).

4 Further Analysis

We have recently extended the analysis of COBE-normalized CDM models to models with general values of Ω and Ω_Λ (Zehavi & Dekel 1998). Although Ω_Λ comes in only indirectly through the COBE normalization, such results are particularly interesting as they can be compared to other constraints in the $\Omega - \Omega_\Lambda$ plane, such as the recent results coming from high-redshift type Ia supernovae (SNe Ia; Perlmutter *et al.* 1998; Riess *et al.* 1998).

Figure 2 illustrates such constraints in the $\Omega - \Omega_\Lambda$ plane, showing $\ln\mathcal{L}$ contours for the SFI catalog, for fixed values of $n = 1$ and $h = 0.65$. The peculiar velocity analysis appears to constrain an elongated ridge in this plane of a nearly fixed Ω and varying Ω_Λ . As demonstrated in the plot, a change in the values of n and h essentially shifts the ridge toward either a higher or lower Ω , for smaller and larger values of these parameters, respectively.

Figure 2 illustrates such constraints in the $\Omega - \Omega_\Lambda$ plane, showing $\ln\mathcal{L}$ contours for the SFI catalog, for fixed values of $n = 1$ and $h = 0.65$. The peculiar velocity analysis appears to constrain an elongated ridge in this plane of a nearly fixed Ω and varying Ω_Λ . As demonstrated in the plot, a change in the values of n and h essentially shifts the ridge toward either a higher or lower Ω , for smaller and larger values of these parameters, respectively.

This is another manifestation of the degeneracy between these parameters mentioned earlier. The acceptable range of these parameters is therefore needed to be determined by other external constraints. The results of the same analysis applied to the Mark III catalog are here as well fairly similar to the SFI ones, except for a slightly stronger preference toward smaller values of Ω_Λ .

The confidence contours in this parameter plane obtained by the Supernova Cosmology Project (Perlmutter *et al.* 1998) are sketched as well in Figure 2. (These results are consistent with the findings of the High-z Supernova Search Team results, Riess *et al.* 1998.) Taking into consideration concurrently these two independent sets of constraints seem to imply a considerable contribution from both Ω and Ω_Λ . While the range of models consistent with the high-z SNe findings alone includes low Ω + low Ω_Λ models (and even $\Omega_\Lambda < 0$), the peculiar velocities analysis appears to rule out these models, and taken together the two make a stronger case for a positive cosmological constant.

Work in progress includes an attempt to merge the Mark III and SFI catalogs and perform a joint likelihood analysis, looking specifically at the cross-correlations of the two data sets, that may entail valuable information. Another aim is to perform a similar analysis on other velocity data, such as velocities of galaxy clusters (e.g., Smith *et al.*, these proceedings) or SNe Ia velocities, which probe out to larger scales with relatively high accuracy. Lastly, an interesting prospect is to do a simultaneous analysis of velocity data together with other kinds of data, like redshift surveys and CMB experiments (see Webster *et al.* 1998; Lahav & Bridle, these proceedings). The distinct types of data complement one another, each constraining different combinations of the cosmological parameters, and together may remove the degeneracy and set tight constraints.

Acknowledgments

I thank my collaborators in this work L.N. da Costa, A. Dekel, A.

Eldar, W. Freudling, R. Giovanelli, M.P. Haynes, Y. Hoffman, T. Kolatt, J.J. Salzer, G. Wegner and S. Zaroubi. This work was supported by the DOE and the NASA grant NAG 5-7092 at Fermilab.

References

da Costa L.N., Freudling W., Wegner G., Giovanelli R., Haynes M.P., Salzer J.J., 1996, ApJ, 468, L5
 da Costa L.N., Nusser A., Freudling W., Giovanelli R., Haynes M.P., Salzer J.J., Wegner G., 1998, MNRAS, 299, 425
 Eldar A. *et al.*, 1998, in preparation
 Freudling W., Zehavi I., da Costa L.N., Dekel A., Eldar A., Giovanelli R., Haynes M.P., Salzer J.J., Wegner G., Zaroubi S., 1998, ApJ, submitted
 Haynes M.P. *et al.*, 1998, in preparation
 Kaiser N., 1988, MNRAS, 231, 149
 Kolatt T., Dekel A., 1997, ApJ, 479, 592
 Kolatt T., Dekel A., Ganon G., Willick, J.A., 1996, ApJ, 458, 419
 Perlmutter S. *et al.*, 1998, LBNL preprint 41801
 Riess A.G. *et al.*, 1998, AJ, in press
 Strauss, M.S., 1998, in Dekel A., Ostriker J.P., eds., *Formation of Structure in the Universe*. Cambridge University Press, Cambridge, p. 172
 Strauss M.A., Willick J.A., 1995, Phys. Rep., 261, 271
 Webster M., Bridle S.L., Hobson M.P., Lasenby A.N., Lahav O., Rocha G., 1998, ApJL, submitted
 Wegner G. *et al.*, 1998, in preparation
 Willick J.A., Courteau S., Faber S.M., Burstein D., Dekel A., 1995, ApJ, 446, 12
 Willick J.A., Courteau S., Faber S.M., Burstein D., Dekel A., Kolatt T., 1996, ApJ, 457, 460
 Willick J.A., Courteau S., Faber S.M., Burstein D., Dekel A., Strauss M.A., 1997, ApJS, 109, 333
 Zaroubi S., Zehavi I., Dekel A., Hoffman Y., Kolatt T., 1997, ApJ, 486, 21
 Zehavi I., Dekel A., 1998, in preparation